









Possible Transient Luminous Events Observed in Jupiter's Upper Atmosphere

Key Points:

- Eleven transient bright flashes were observed by the ultraviolet instrument on the Juno mission
- The flashes have an average duration of 1.4 ms, are located 260 km above the 1-bar level and are dominated by H₂ emission
- The observations are consistent with transient luminous events which occur in the upper atmosphere in response to tropospheric lightning

Rohini S. Giles¹ , Thomas K. Greathouse¹ , Bertrand Bonfond² , G. Randall Gladstone^{1,3} , Joshua A. Kammer¹ , Vincent Hue¹ , Denis C. Grodent³, Jean-Claude Gérard³ , Maarten H. Versteeg¹ , Michael H. Wong^{4,5} , Scott J. Bolton¹ , John E. P. Connerney^{6,7} , and Steven M. Levin⁸ 

¹Space Science and Engineering Division, Southwest Research Institute, San Antonio, TX, USA, ²Laboratoire de Physique Atmosphérique et Planétaire, STAR Institute, Université de Liège, Liège, Belgium, ³Department of Physics and Astronomy, University of Texas at San Antonio, San Antonio, TX, USA, ⁴Department of Astronomy, University of California, Berkeley, CA, USA, ⁵SETI Institute, Mountain View, CA, USA, ⁶Space Research Corporation, Annapolis, MD, USA, ⁷Goddard Space Flight Center, Greenbelt, MD, USA, ⁸Jet Propulsion Laboratory, Pasadena, CA, USA

Correspondence to:

R. S. Giles,
rgiles@swri.edu

Citation:

Giles, R. S., Greathouse, T. K., Bonfond, B., Gladstone, G. R., Kammer, J. A., & Hue, V., et al. (2020). Possible transient luminous events observed in Jupiter's upper atmosphere. *Journal of Geophysical Research: Planets*, 125, e2020JE006659. <https://doi.org/10.1029/2020JE006659>

Received 19 AUG 2020
Accepted 6 OCT 2020

Abstract Eleven transient bright flashes were detected in Jupiter's atmosphere using the ultraviolet spectrograph instrument on the Juno spacecraft. These bright flashes are only observed in a single spin of the spacecraft and their brightness decays exponentially with time, with a duration of ~1.4 ms. The spectra are dominated by H₂ Lyman band emission and based on the level of atmospheric absorption, we estimate a source altitude of 260 km above the 1-bar level. Based on these characteristics, we suggest that these are observations of transient luminous events (TLEs) in Jupiter's upper atmosphere. In particular, we suggest that these are elves, sprites or sprite halos, three types of TLEs that occur in the Earth's upper atmosphere in response to tropospheric lightning strikes. This is supported by visible light imaging, which shows cloud features typical of lightning source regions at the locations of several of the bright flashes. TLEs have previously only been observed on Earth, although theoretical and experimental work has predicted that they should also be present on Jupiter.

Plain Language Summary The Juno spacecraft has been in orbit around Jupiter since 2016. One of the instruments on this spacecraft is an ultraviolet spectrograph (UVS), which is primarily used to make ultraviolet images of Jupiter's auroras. During the first 4 years of the mission, the UVS has observed 11 transient bright flashes. These bright flashes look similar to lightning, but are located much higher in the atmosphere than the cloudy regions of Jupiter where lightning is generated. We suggest that these are observations of transient luminous events (TLEs) in Jupiter's upper atmosphere. In particular, we suggest that these are elves, sprites or sprite halos, three types of TLEs that produce spectacular flashes of light very high in the Earth's atmosphere in response to lightning strikes between clouds or between clouds and the ground. TLEs have previously only been observed on Earth, although theoretical and experimental work has predicted that they should also be present on other planets, including Jupiter. Comparing and contrasting TLE observations between Jupiter and Earth will improve our understanding of electrical activity in planetary atmospheres.

1. Introduction

Lightning in Jupiter's atmosphere was first observed with instruments on the Voyager 1 spacecraft; the imaging camera recorded optical flashes on the nightside of the planet (Cook et al., 1979; Smith et al., 1979), while the plasma wave instrument measured low-frequency whistler waves, which on Earth are associated with lightning (Gurnett et al., 1979). Optical imaging instruments on subsequent missions have also made observations of lightning, including Voyager 2 ISS (Borucki & Magalhaes, 1992), Galileo SSI (Little et al., 1999), Cassini ISS (Dyudina et al., 2004), and New Horizons LORRI (Baines et al., 2007). In addition to these visible-light observations, the lightning and radio emissions detector on the Galileo entry probe also recorded radio emission with a similar waveform to Earth lightning discharge (Rinnert et al., 1998).

The most recent spacecraft to have detected lightning in Jupiter's atmosphere is the Juno mission, which has been in orbit around Jupiter since 2016 (Bolton et al., 2017). Three Juno instruments have reported observations of lightning. The microwave radiometer (MWR) detected almost 400 lightning events in the

2016–2018 time period (Brown et al., 2018). These detections were in the form of discrete impulses, measured at a frequency of 600 MHz and were interpreted as lightning sferics, broadband electromagnetic impulses that result from lightning discharge. In addition to these sferics, the radio and plasma wave instrument (Waves) has detected thousands of low-frequency (<20 kHz) whistler waves (Kolmasová et al., 2018). On 11 occasions, sferics and whistler waves were observed concurrently by MWR and Waves, marking the first time that lightning in Jupiter's atmosphere has been simultaneously observed by multiple instruments (Imai et al., 2018). The third instrument that has so far reported lightning observations is the Stellar Reference Unit (SRU), a low light visible imager designed for attitude determination. As with previous optical observations, the SRU lightning detections consist of bright flashes on the planet's nightside (Becker et al., 2020).

Lightning observed in Jupiter's atmosphere has generally been thought to originate in the planet's water cloud layer, in an analogous manner to intracloud lightning on Earth (Levin et al., 1983). Borucki and Williams (1986) found that the Voyager 1 optical images were best modeled when the lightning was assumed to occur within a cloud at 5 bar, the estimated location of the water cloud. During the Galileo observations, lightning on the nightside was directly linked to a storm that was imaged on the dayside; analysis of the stormcloud suggested it was located at >4 bars (Little et al., 1999). Kolmasová et al. (2018) also suggested that the lightning observations made by the Juno Waves instrument are likely to originate in Jupiter's water cloud, based on the similar flash density to terrestrial lightning. However, recent observations by the Juno SRU have shown that the lightning processes on Jupiter are more complex than previously thought. Becker et al. (2020) found that some of the lightning observed by the SRU occurs at pressures of 1.4–1.9 bar, where pure liquid water cannot exist. Instead, they suggest that a mixed ammonia-water liquid plays an important role in generating this “shallow” lightning.

While lightning has been observed many times on both Jupiter and other planets in the solar system (Dyudina et al., 2010; Zarka & Pedersen, 1986), there are other atmospheric electricity phenomena that have thus far only been observed in the Earth's atmosphere. Transient luminous events (TLEs) are large-scale bright events that occur in the Earth's upper atmosphere and are linked to the electrical activity in an underlying storm system (Pasko, 2010). After many years of eyewitness accounts, a serendipitous observation of a TLE was first recorded in 1989 (Franz et al., 1990). Since that time, there have been numerous observation campaigns from both the ground (e.g., Gordillo-Vázquez et al., 2018; Kanmae et al., 2007) and from space-based instruments (e.g., Chern et al., 2003; Sato et al., 2015). These observations have allowed different types of TLEs to be identified, including elves, sprites, sprite halos, and blue jets (Pasko, 2010). Each of these has a different visual appearance and is driven by a different production mechanism.

In this paper, we report on bright, lightning-like flashes observed by the ultraviolet spectrograph (UVS) on Juno. This is the first time that a Jovian lightning-like phenomenon has been observed in the ultraviolet. These bright flashes are notably different from previous observations of lightning, because Jupiter's atmosphere is optically thick in the ultraviolet, so observations cannot probe beneath the 100-mbar level (Vincent et al., 2000). Any bright flashes detected by UVS therefore must occur much higher in the atmosphere than both the water cloud and the “shallow” lightning observed by Becker et al. (2020), and must be driven by a different mechanism than intracloud discharge. In this paper, we conclude that these bright flashes are consistent with TLEs in Jupiter's upper atmosphere, a phenomenon that has been predicted for Jupiter (Yair et al., 2009) but has not been previously observed.

In Section 2, we describe the Juno UVS instrument and the method of detection of the bright flashes. Section 3 describes the analysis of the bright flashes: their spatial extent, light curves, and spectra. Finally, Section 4 discusses these results and compares them to theoretical predictions for TLEs in Jupiter's atmosphere.

2. Observations

2.1. Juno UVS

The UVS is a far-ultraviolet imaging spectrograph on NASA's Juno mission (Gladstone, Persyn, et al., 2017). UVS covers the 68–210 nm spectral range with a spectral resolution that varies between 1.3 and 3.0 nm depending on the position along the instrument's slit (Greathouse et al., 2013). The primary scientific

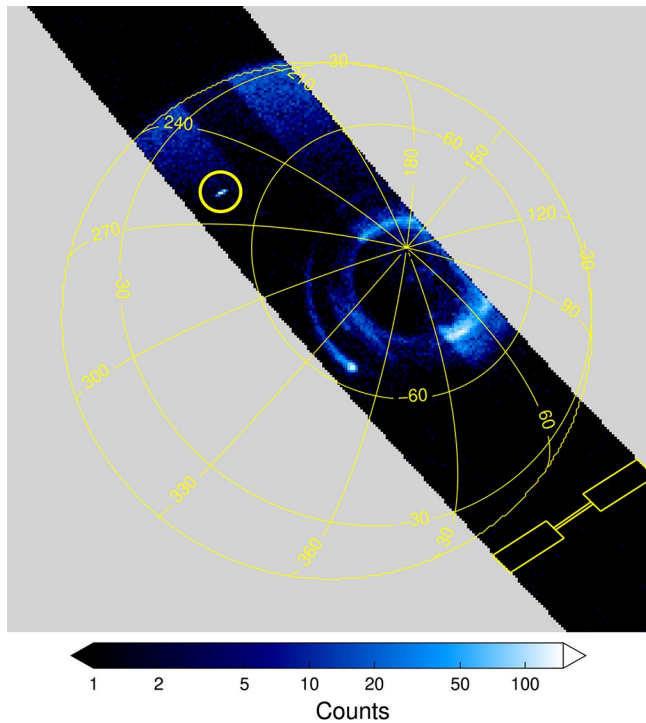


Figure 1. A spatial map of Juno ultraviolet spectrograph measurements during a single spacecraft spin at PJ26 (10 April 2020). The color scale shows the number of photons counts measured. The shape of the instrument slit is shown in yellow in the lower right corner (widths of the both the wide and narrow slits increased by a factor of 5 for clarity). A bright flash is highlighted by the yellow circle. This flash is also shown in Figure 2j.

goal of the UVS instrument is to characterize the morphology, brightness, and spectral characteristics of Jupiter's far-ultraviolet auroral emission and this spectral range includes the H Lyman series and the Lyman, Werner, and Rydberg band systems of H_2 .

Juno is a spin-stabilized spacecraft with a rotation period of ~ 30 s. The UVS instrument slit is nominally parallel to the spacecraft's spin axis, but can be pointed away by up to $\pm 30^\circ$ by using the scan mirror. Photons that enter the instrument slit register as a pulse on the microchannel plate detector. High energy electrons and ions that are present in Jupiter's high radiation environment also register as individual pulses and add noise to the UVS data. UVS data are recorded in a pixel-list time-tagged format; for each photon detection, the x and y position on the detector and the time of the detection are recorded. The x position provides the wavelength of the photon. The y position provides the position along the slit, and this can be combined with the spin phase of the spacecraft at the time of observation in order to assign a position on the planet to each photon. This geometric information can then be used to produce spatial maps of the ultraviolet radiation (e.g., Gladstone, Versteeg, et al., 2017). The UVS slit is made up of two wide segments on either side of one narrow segment, as shown in Figure 1. The wide slit has an angular width of 0.2° , which means that a point source is within the field of view for 17 ms as the spacecraft rotates, and the narrow slit has a width of 0.025° . The full width at half maximum (FWHM) across the slit is larger than the actual slit size: for the wide part of the slit, it is $\sim 0.25^\circ$ and for the narrow part of the slit it is $\sim 0.2^\circ$ (Greathouse et al., 2013).

The Juno spacecraft is in a highly elliptical orbit around Jupiter, and UVS obtains high spatial resolution observations of Jupiter for several hours on either side of each perijove (PJ), the point of closest approach to the planet. Data acquisition is paused when the spacecraft passes through regions of Jupiter's radiation belts where the background count rate from high energy electrons and ions overwhelms the count rate from UV photons (Kammer et al., 2018). As Juno's orbit precesses over the course of the mission, the PJ location has moved further north. This means that observations of the north polar region have a higher spatial resolution, but are obtained over a shorter time period and have higher background radiation. Observations of the south pole are decreasing in spatial resolution, but are being obtained over a long time period and are more clear of radiation (Gladstone et al., 2019).

2.2. Observations of Bright Flashes

The Juno UVS team produces spatial maps of Jupiter for each spin of the spacecraft during each PJ. An example maps for a single spin during PJ26 (10 April 2020) is shown in Figure 1. The image swath is built up as the instrument slit sweeps over the planet as the spacecraft rotates. Figure 1 is centered on Jupiter's south pole, and the data were obtained as the spacecraft was moving away from the planet.

The brightest features in Figure 1 are the southern auroral oval and the Io footprint, both of which are within 30° of the pole. During this spin, another bright feature was detected at a (planetocentric) latitude of $51.0^\circ S$ and a longitude of $258.7^\circ W$; this bright feature is highlighted by the solid yellow circle in Figure 1. Unlike the auroral emission, this bright spot was very transient. It was not present in the previous or subsequent spins (± 30 s), and as discussed in the following sections, the very short extent in the spin direction indicates that the bright spot is even more short-lived than that.

Data from all PJs were analyzed to search for comparable short-lived bright flashes. Photon detections within a localized ($\pm 0.4^\circ$) region along the slit were binned into a 5-ms intervals. Bin X was flagged if its count rate was 15 times higher than both bin $X - 1$ and bin $X + 2$, and was also at least 50. The photon detection

Table 1
Eleven Bright Flashes Observed by Juno Ultraviolet Spectrograph

Date	Time	Lat (°)	Lon (°)	Solar zenith angle (°)	Wind shear	Spacecraft distance (km)	Slit	Max width (km)	Duration (ms)	Energy (J)	
(a)	27 August 2016	14:35:15	−43.2	353.7	99	Cyclonic	172,000	Wide	750	0.8	2.2×10^7
(b)	27 August 2016	14:57:16	−43.3	350.2	88	Cyclonic	201,000	Wide	1,280	1.6	2.0×10^8
(c)	02 September 2017	00:34:16	−51.2	236.3	103	Cyclonic	255,000	Wide	1,350	1.3	2.1×10^8
(d)	02 September 2017	00:39:48	−43.0	263.2	119	Cyclonic	269,000	Wide	1,310	1.3	1.9×10^8
(e)	16 December 2017	17:09:14	34.0	165.7	137	Cyclonic	103,000	Wide	660	2.5	1.8×10^7
(f)	07 September 2018	05:06:16	−27.4	248.8	93	Cyclonic	367,000	Narrow	1,810	1.9	1.3×10^9
(g)	29 May 2019	09:17:24	−61.6	222.5	110	Anticyclonic	127,000	Wide	810	0.8	4.4×10^7
(h)	26 December 2019	19:03:20	−66.3	166.9	73	Cyclonic	133,000	Wide	920	0.1	5.3×10^7
(i)	10 April 2020	13:00:42	52.8	216.1	123	Cyclonic	72,000	Wide	490	1.3	2.8×10^6
(j)	10 April 2020	17:24:35	−51.0	258.7	86	Cyclonic	338,000	Wide	1,930	1.4	5.0×10^8
(k)	25 July 2020	10:37:13	−69.0	239.9	106	-	385,000	Wide	2,180	1.4	1.9×10^8

Note. The times are given to the closest second and are as measured on the spacecraft. Latitudes are planetocentric and longitudes are System III West. The wind shear describes whether the winds are cyclonic or anticyclonic at the latitude of the observations (observation [k] occurred too close to the pole for the wind shear to be measured). The spacecraft distance is the distance from the bright flash to the spacecraft. The slit column indicates whether the observation was made in the wide part of the slit or the narrow part of the slit. The widths are discussed in Section 3.1, the durations are discussed in Section 3.2, and the energies are discussed in Section 3.3.

histograms for the flagged events were then manually inspected; in some cases, the spike in photon detections was due to auroral emission (evident from the spatial location and a high average count rate over a >20 ms time interval) or bar code radiation events (evident from abrupt changes in the count rate that affect the entire slit equally, Bonfond et al., 2018). Through this process, we found a total of 11 events that consist of short-lived, spatially localized bright flashes. These 11 events are listed in Table 1 and are analyzed in Section 3.

3. Results

3.1. Images

Figure 2 shows images of the 11 events listed in Table 1. As described in Section 2.1, Juno UVS images are generated by the instrument slit sweeping across the planet as the spacecraft rotates. These images were made by mapping the detected photons into $0.1^\circ \times 0.1^\circ$ bins on the sky and each image is 10×10 bins ($1^\circ \times 1^\circ$). As they have been mapped onto the sky, the images each have different orientations relative to the slit. In each case, the slit direction is parallel to the streak direction, and the spin direction is approximately perpendicular ($\pm 30^\circ$) to the streak direction. For example, in Figure 2b the slit is oriented horizontally and in Figure 2h the slit is oriented vertically. As noted in Table 1, some of the observations (b), (h), and (j) were made on the dayside of the planet, but the bright flashes are still clearly visible above the background reflected sunlight.

We used a 2-d Gaussian fitting routine (Markwardt, 2009) to measure the sizes of the bright regions in Figure 2. In the across-slit direction, the FWHM is less than 0.1° in all cases. For a constant point source, the measured FWHM across the slit is $0.2\text{--}0.3^\circ$ (Greathouse et al., 2013). The fact that the measured FWHM is narrower suggests a temporal effect, and this is explored in more detail in Section 3.2. In the along-slit direction, the measured FWHM is $0.33 \pm 0.05^\circ$. When we consider the distance to the spacecraft during each of these measurements (Table 1), this equates to widths of 500–2,200 km. However, a FWHM of $\sim 0.3^\circ$ is also consistent with the point spread function of the instrument (Greathouse et al., 2013), so the source regions could also be considerably smaller than these maximum width values.

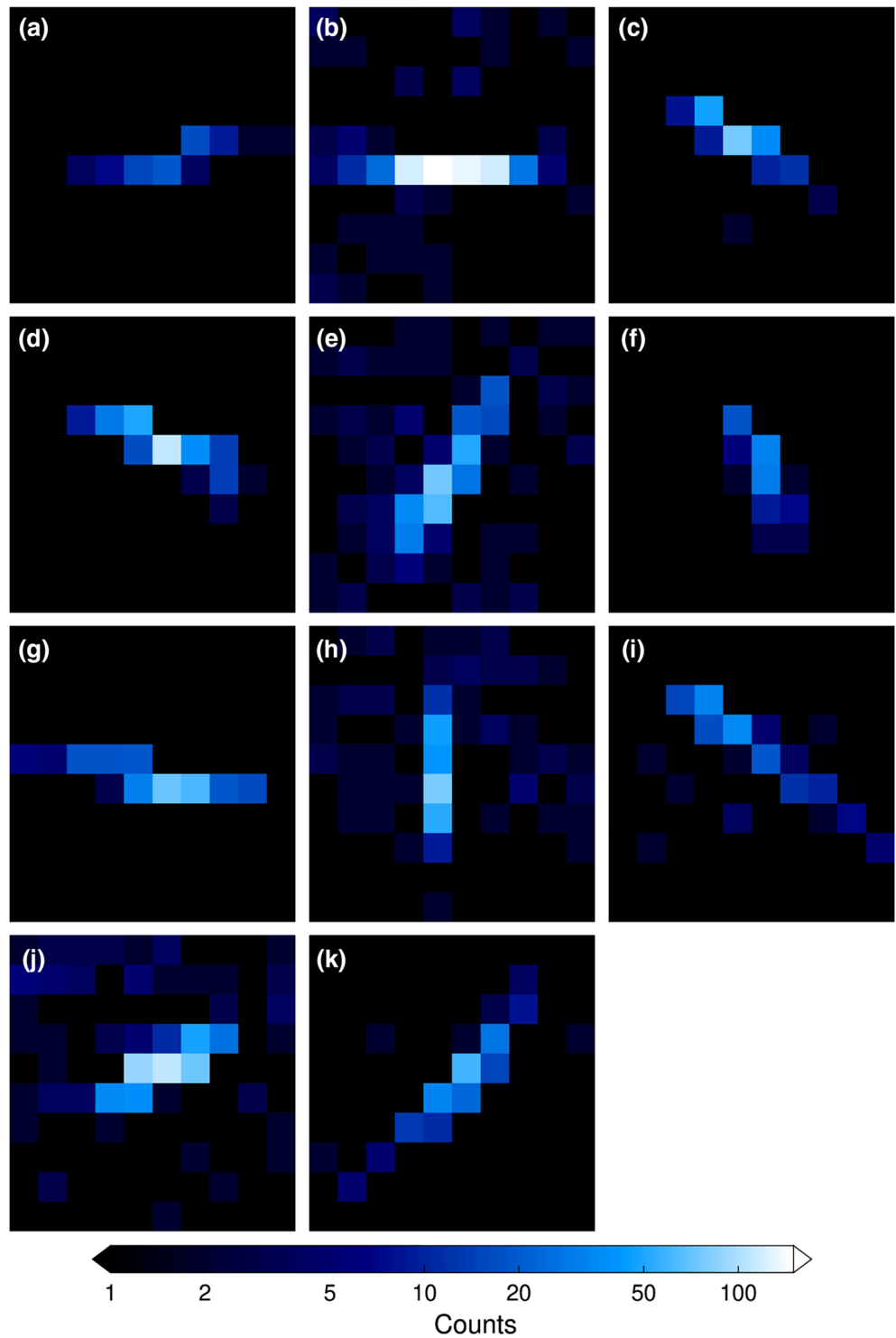


Figure 2. Images of 11 bright flashes observed by Juno ultraviolet spectrograph. The labels relate the images to the bright flashes described in Table 1. The color scale shows the number of photons counts measured. Each image has dimensions $1^\circ \times 1^\circ$ on the sky. Panel (j) shows the same bright flash as Figure 1.

Table 2
Types of Transient Luminous Events Observed in the Earth's Upper Atmosphere

Type	Mechanism	Shape/size	Altitude	Duration
Blue jets	Discharge between the upper positive charge region in a thundercloud and a negative layer above the cloud	Narrow cone of light extending upwards, ~3 km wide	From cloud tops to 50 km	~250 ms
Sprites	A cloud-to-ground lightning strike generates a quasielectrostatic field above the cloud, which accelerates electrons and leads to N ₂ emission	Set of luminous columns with a total width of 25–50 km, tendrils extending downwards	50–90 km	>5 ms
Sprite halos	As with sprites, they are caused by quasielectrostatic thundercloud fields; they sometimes precede the more structured sprites	Diffuse disk-shaped emission with a diameter of <100 km	70–85 km	2–10 ms
Elves	An intense cloud-to-ground lightning strike causes an upward moving electromagnetic pulse, which heats ambient electrons and leads to N ₂ emission	Diffuse and ring-shaped, up to 300 km wide	75–105 km	<1 ms

Note. Information obtained from Rodger (1999), Pasko (2010), and Gordillo-Vzquez et al. (2011).

These images provide evidence that these observations were due to UV photons from Jupiter, rather than the result of radiation noise. If the hundreds of detected events measured by the instrument were due to a sudden increase in the number of background radiation counts, we would expect the counts to be distributed randomly along the slit, as shown in Bonfond et al. (2018), rather than clustered spatially in a Gaussian shape along the slit.

3.2. Light curves

Figure 3 shows the light curves for the 11 events listed in Table 1. Each frame shows the rate of photon detection as a function of time, as the UVS slit scanned over the planet. Because of the finite slit width, a steady point source will remain within the field-of-view of the wide slit for 17 ms (2 ms for the narrow slit). Ten out of the 11 events listed in Table 1 were observed in the wide slit, and yet the events shown in Figure 3 all have shorter durations than 17 ms. This immediately suggests that the source has a brightness that varies on <17 ms timescales.

The shapes of these events appear to be pulses that decay exponentially with time. We fit the distributions using the convolution of a Gaussian with an exponential decay. The width of the Gaussian was held fixed at 0.2 ms, the value that provided the collective best fit for all 11 events. With this Gaussian width, the fitted exponential decay times are listed in Table 2.

The light curves shown in Figure 3 may not represent the complete light curve for each event; either the beginning or the end of the light curve could fall outside the 17 ms interval during which the source is observable. Figure 3h has a noticeably narrower shape than the other figures and the fitted decay times is very short (0.1 ms). One possibility may be that the pulse onset occurred immediately before the slit moved off the source, so the decay phase was not captured. For the remaining 10 events, the mean decay time is 1.4 ± 0.5 ms.

3.3. Energy

We estimated the total energy emitted by the bright source region as follows, based on Hue, Greathouse, et al. (2019):

$$E = f \times \sum_{\lambda=155}^{162} 4\pi d^2 \frac{hc}{\lambda} \sum_{x,y} C_{x,y}^{\lambda} \Omega_{x,y} \quad (1)$$

As described in Section 3.1, we produce UV maps by binning recorded photons into $0.1^\circ \times 0.1^\circ$ bins on the sky. In Equation 1, these bins are labeled with x and y coordinates. We also bin the photons into 0.6 nm wavelength bins, in order to produce a three-dimensional image cube, where $C_{x,y}^{\lambda}$ is the number of photon counts in a wavelength bin λ , per solid angle, per detector area.

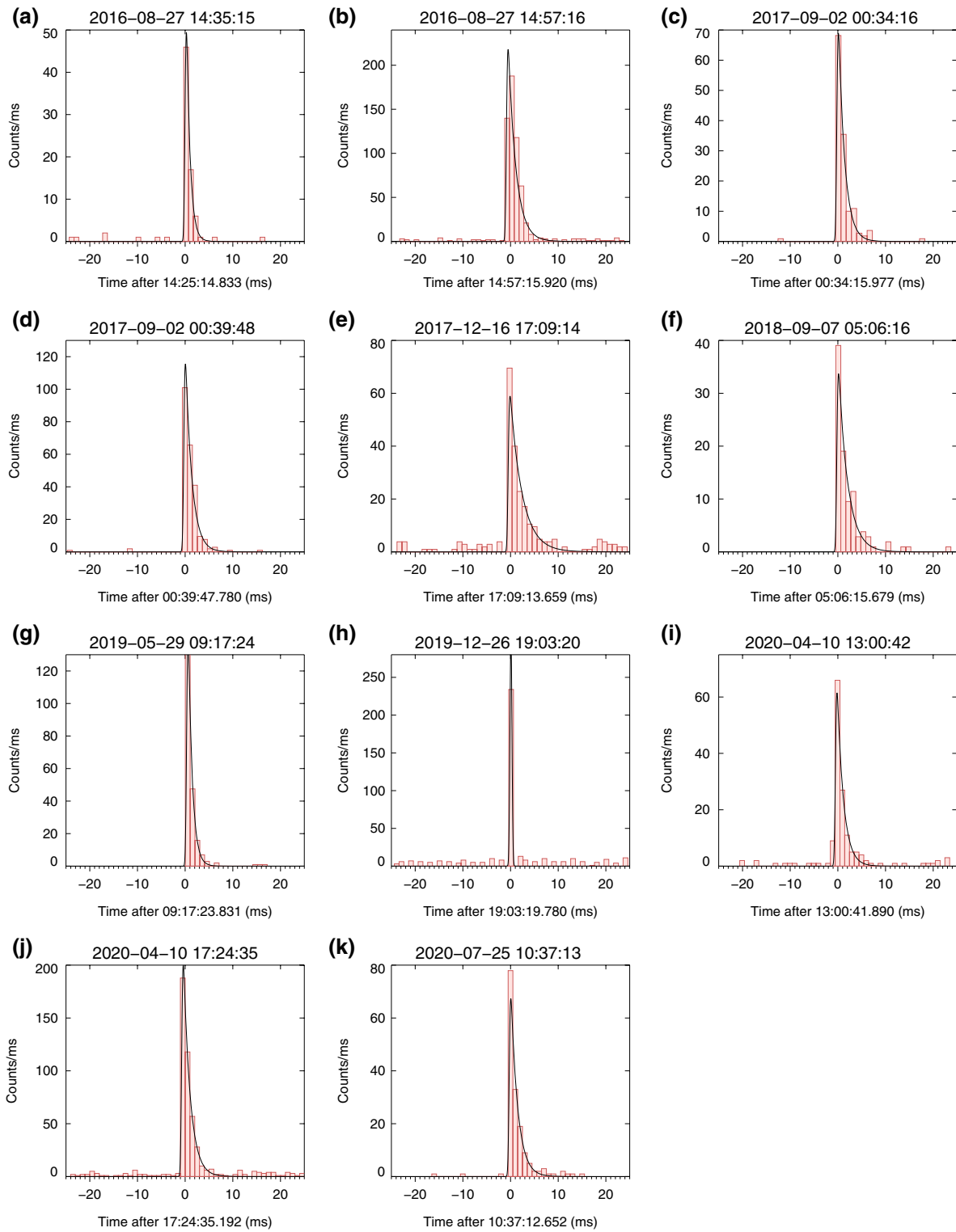


Figure 3. Light curves of 11 bright flashes observed by Juno ultraviolet spectrograph. The labels relate the light curves to the bright flashes described in Table 1. A histogram of the photon detections is shown in red; bin widths were chosen to produce a smooth distribution and vary slightly between the different frames. A fitted Gaussian-exponential convolution is shown in black for each event.

To convert this image cube into the total energy, we first multiply $C_{x,y}^{\lambda}$ by the solid angle of each x,y bin ($0.1^{\circ} \times 0.1^{\circ}$) and then sum over the small spatial region containing the bright flash (Figure 2). h and c are the Planck constant and the speed of light, and are used to convert the photon detections into energy. d is the distance between the bright flash and the spacecraft when the observations were made, and is used to convert between radiant exposure and radiant energy, assuming photons are emitted isotropically.

In order to calculate the total H₂ emission, we follow the method described in Bonfond et al. (2017). We first sum over photons in the 155–162 nm spectral range, a wavelength range selected because there is negligible atmospheric absorption in the upper atmosphere (see Section 3.4 for a discussion about the source altitude). Based on a synthetic spectrum, this summed value is then multiplied by $f = 8.1$ in order to scale it to the whole H₂ Lyman and Werner bands UV spectrum.

The final H₂ emission energies are in the 10^6 – 10^9 J range (see Table 1). The systematic and random errors are at least 20% (Gérard et al., 2019), and the calculated values are also very dependent of the assumption of isotropic emission.

3.4. Spectra

Figure 4 shows the spectra for the 11 events listed in Table 1. These spectra were calculated in a similar manner to the total energy calculation in Section 3.3. To convert from radiant energy density to spectral irradiance, we divided each spectrum by the exponential decay times calculated in Section 3.2. The final spectra are presented in terms of spectral irradiance at the spacecraft location, that is, W/cm²/nm. The spectra have been smoothed using a 2-nm boxcar and they have been background-subtracted to limit the effect of reflected sunlight at the longest wavelengths. The error bars in Figure 4 were calculated combining shot noise (a signal-to-noise ratio of \sqrt{N} , where N is the number of photon counts recorded) and radiation noise (calculated from the average count rate at <80 nm, where we expect the counts to all be due to radiation).

Individually, each of the spectra shown in Figure 4 are somewhat noisy, but it is clear that they do share some broad spectral features, particularly a double peak at 160 nm. In order to conduct further analysis, we combine spectra (a), (c), (d), (e), (g), (i), and (k) into a single spectrum with a higher signal-to-noise ratio. These are the cleanest spectra, as the observations were made within the wide slit where the signal-to-noise ratio is higher and they were made on the nightside of the planet, so there is no reflected sunlight. This combined spectrum is shown in black in Figure 5.

Figure 5 shows that the bright flash spectrum has a strong double peak at 160 nm, with the irradiance decreasing at both shorter and longer wavelengths. This peak matches the location of a double peak in the H₂ Lyman band that is prominent in observations of Jupiter's auroral emission (Gustin et al., 2004), immediately suggesting that H₂ emission also plays a significant role in the bright flash spectrum. This spectrum conclusively demonstrates that the bright flashes are not due to radiation noise, as counts from radiation would be randomly distributed in the spectral direction and would produce a featureless spectrum that varies with the effective area of the instrument (Hue, Gladstone, et al., 2019).

In order to compare the possible H₂ emission in the bright flash spectrum with the auroral H₂ emission, the red line in Figure 5 shows an auroral spectrum from Jupiter, obtained by combining wide-slit Juno UVS data from many PJs. This auroral spectrum has been binned in the same manner as the bright flash spectrum, although we note that the UVS spectral resolution varies along the slit and therefore the two spectra will not have exactly the same spectral resolution. The auroral spectrum has also been scaled to match the peak irradiance of the bright flash spectrum. The auroral and bright flash spectra both show the same H₂ emission peak at 160 nm, and have a similar spectral shape in the 155–180 nm range. However, at shorter wavelengths, the auroral emission from H₂ is brighter. By 125–130 nm, this difference is approximately an order of magnitude. This suggests that the bright flash has higher absorption from gases such as CH₄ and C₂H₂ which absorb strongly at these shorter wavelengths, in turn suggesting that the bright flash emission originates from deeper in the atmosphere.

In order to study this further, we used a model of Jupiter's atmosphere to determine how atmospheric absorption affects the shape of H₂ Lyman band emission. The three stratospheric gases that contribute significantly to absorption in the 125–180 nm range are CH₄, C₂H₂, and C₂H₆. CH₄ absorption cross-sections were

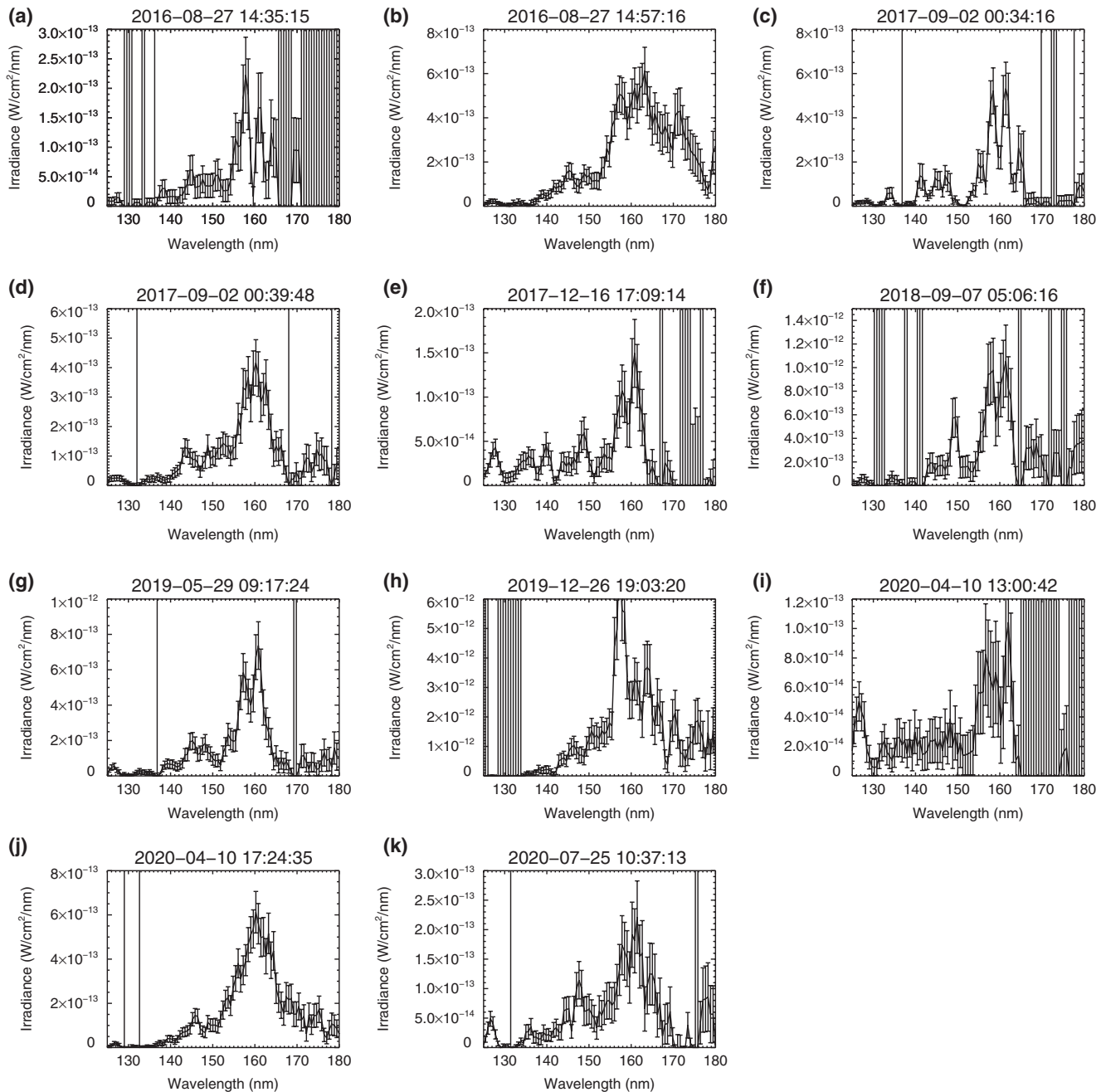


Figure 4. Spectra of 11 bright flashes observed by Juno ultraviolet spectrograph. The labels relate the spectra to the bright flashes described in Table 1. Error bars combine shot noise and radiation noise.

obtained from Chen and Wu (2004) and Lee et al. (2001), C_2H_2 was obtained from Bénilan et al. (2000) and Smith et al. (1991), and C_2H_6 was obtained from Lee et al. (2001). For a given altitude, the column density of each gas was calculated using the atmospheric composition model described by Model C in Moses et al. (2005). The column densities and absorption cross-sections were used to calculate the atmospheric transmission from the given altitude level. This was then multiplied by an H_2 model from Gustin et al. (2004) to produce a top-of-atmosphere spectrum, which was then smoothed to match the Juno UVS observations.

This model was used to iteratively fit the observed bright flash spectrum with two free parameters: the source altitude and a scaling factor. The best fit result is shown by the red line in Figure 6 and the corresponding source altitude is 258 ± 10 km above the 1-bar level (10 bar). The blue line shows the case where

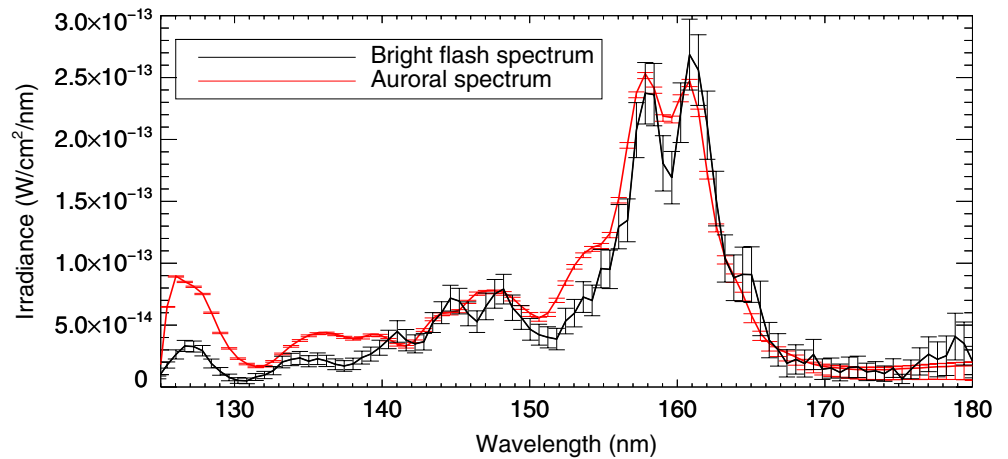


Figure 5. The averaged spectrum (black) of the seven cleanest Juno ultraviolet spectrograph (UVS) bright flash observations (a, c–e, g, i, and k from Figure 4). For comparison, a spectrum of Jupiter’s aurora as seen by Juno UVS is shown in red (scaled to match the peak irradiance).

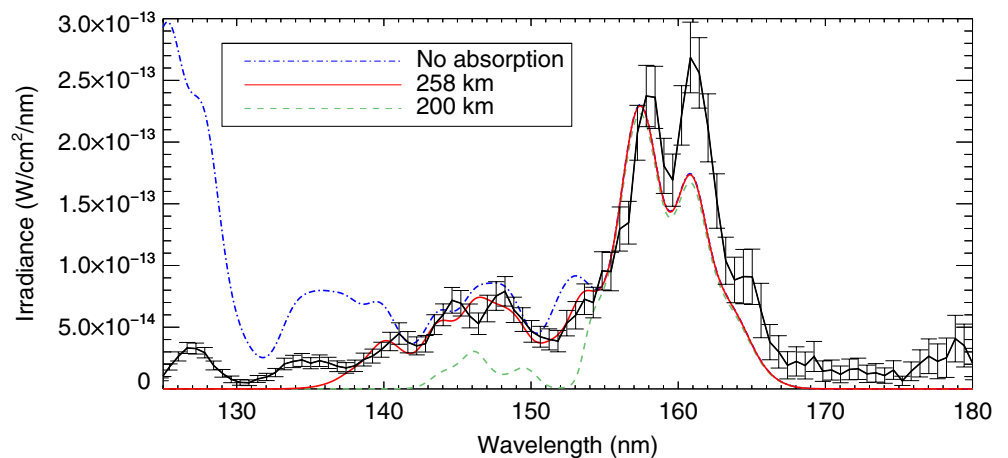


Figure 6. Modeling the bright flash spectrum as H₂ emission attenuated by atmospheric absorption. The best fit model is shown in red, and corresponds to a source altitude of 258 km above the 1-bar level. For comparison, we show the spectrum of a source with no atmospheric absorption (blue) and a source located deeper in the atmosphere, at 200 km (green).

there is no atmospheric absorption, and the green line shows the case where the source is located deeper in the atmosphere, at an altitude of 200 km, so there is more atmospheric absorption. The blue line is far too bright in the 125–140 nm range, while the green line is too dim at 140–150 nm. In contrast, the best fit red line provides a good fit to the observations throughout the 125–160 nm range. At >160 nm, the model does not provide a good fit to the bright flash spectrum; given the similarity between the bright flash spectrum and the auroral spectrum shown in Figure 5, the same discrepancy exists between the model and the auroral spectrum. One possible explanation for this is the presence of H₂ *a–b* continuum emission which peaks in the 200–250 nm range but also extends to shorter wavelengths (Pryor et al., 1998) and is not included in the Gustin et al. (2004) model.

4. Discussion and Conclusions

The events described in Section 3 and listed in Table 1 have the following properties:

- (1) They are consistent with point sources (maximum widths of 500–2,200 km)
- (2) Their brightness decays exponentially with time, with a decay time of ~1.4 ms

- (3) They are dominated by H₂ emission
- (4) Their total Lyman and Werner band H₂ energy output is in the 10⁶–10⁹ J range
- (5) They are located at an altitude of ~260 km above the 1-bar level (at a pressure of 10 μbar).

The transient nature and very short decay time of the bright flashes is reminiscent of lightning. However, lightning in Jupiter's atmosphere is generally thought to occur in Jupiter's water cloud layer at ~5 bar (Levin et al., 1983) and even the recently observed “shallow lightning” occurs at pressures >1.4 bar (Becker et al., 2020). Ultraviolet observations in contrast cannot probe below 100 mbar (Vincent et al., 2000), and our analysis shows that the bright flashes are located ~260 above the 1-bar region, which corresponds to ~300 km above the location of the water cloud. It is therefore clear that we are not observing typical cloud-to-cloud lightning strikes. Instead, we suggest that these bright flashes may be upper atmospheric responses to underlying lightning storms, similar to what is seen in the Earth's upper atmosphere.

As discussed in Section 1, TLEs are atmospheric electricity phenomena in the Earth's upper atmosphere, which are caused by lightning discharges. There are several different types of TLEs, including sprites, sprite halos, elves, and blue jets. Each of these has different characteristics and a different mechanism, and these are summarized in Table 2. Blue jets emerge directly from the tops of thunderclouds, so are located deeper in the atmosphere than the other types of TLEs, and they also last ~250 ms. For both of these reasons, they seem inconsistent with our observations. However, sprites, sprite halos and elves occur higher in the atmosphere and have shorter durations, so seem to be plausible candidates.

Sprites, sprite halos and elves have a similar generation mechanism; in each case, a strong tropospheric lightning strike leads to the acceleration of ambient electrons in the upper atmosphere. In the case of sprites and sprite halos, this is thought to be due to the presence of a quasielectrostatic field above the cloud tops that accelerates either ambient or high energy electrons produced from cosmic rays, and in the case of elves, this is thought to be due to an upward propagating electromagnetic pulse. In both cases, this leads to the collisional excitation of N₂ molecules, the primary constituent of the Earth's atmosphere (Rodger, 1999).

TLEs have so far only been detected in the Earth's atmosphere, although recent theoretical and laboratory studies have suggested that they may be present on other planets. The possibility was first raised by Yair et al. (2009), who predicted that sprites could occur in Jupiter's upper atmosphere and that their spectra would be dominated by hydrogen emission since that is the primary constituent of Jupiter's atmosphere. This was further confirmed by Dubrovin et al. (2010), who conducted laboratory experiments to show that sprite-like discharges in a Jupiter-like atmosphere are dominated by H and H₂ emission. Yair et al. (2009) developed a quasielectrostatic model of Jupiter's atmosphere, and using that, they predicted that Jovian sprites would be ignited at an altitude of ~280 km. The possibility of elves in Jupiter's atmosphere has been studied by Luque et al. (2014) and Pérez-Invernón et al. (2017). Luque et al. (2014) estimated that for Jupiter the peak photon density for elves would be at an altitude of 250–300 km, and Pérez-Invernón et al. (2017) found that the width of elves in Jupiter's atmosphere could be between ~400 km for horizontal discharge and ~800 km for vertical discharge. For both sprites and elves, the characteristic decay times can vary from submillisecond to several milliseconds, depending on the parameters used in the model (Dubrovin et al., 2014; Luque et al., 2014).

Based on these properties, it is difficult to determine whether our observations are more consistent to be sprites/sprite halos (quasielectrostatic field generated) or elves (electromagnetic pulse generated). On Earth, the primary distinguishing characteristics are the width, the vertical extent and the duration. Our observed widths are broadly consistent with predictions for all three (although the largest elve predictions slightly exceed our smallest maximum width measurements), and we do not have information on the vertical extents. Our measured duration of ~1.4 ms is similar to the duration of sprite halos of Earth, and is also broadly consistent with the range of values obtained from Jupiter models of sprites and elves.

On Earth, sprites, sprite halos and elves can only be generated in conjunction with a lightning strike. If our observations are indeed one of these TLEs, we would therefore expect there to be a tropospheric lightning flash immediately beforehand. As discussed in Section 1, there are several other instruments on the Juno mission that have previously observed lightning in Jupiter's atmosphere. Unfortunately, none of these instruments observed lightning at the same time as the 11 events we measured with UVS. This is not unexpected, given the manner in which the different observations are all obtained. The Waves instrument detects whistler waves that propagate from the planet to the spacecraft along the magnetic field lines and makes

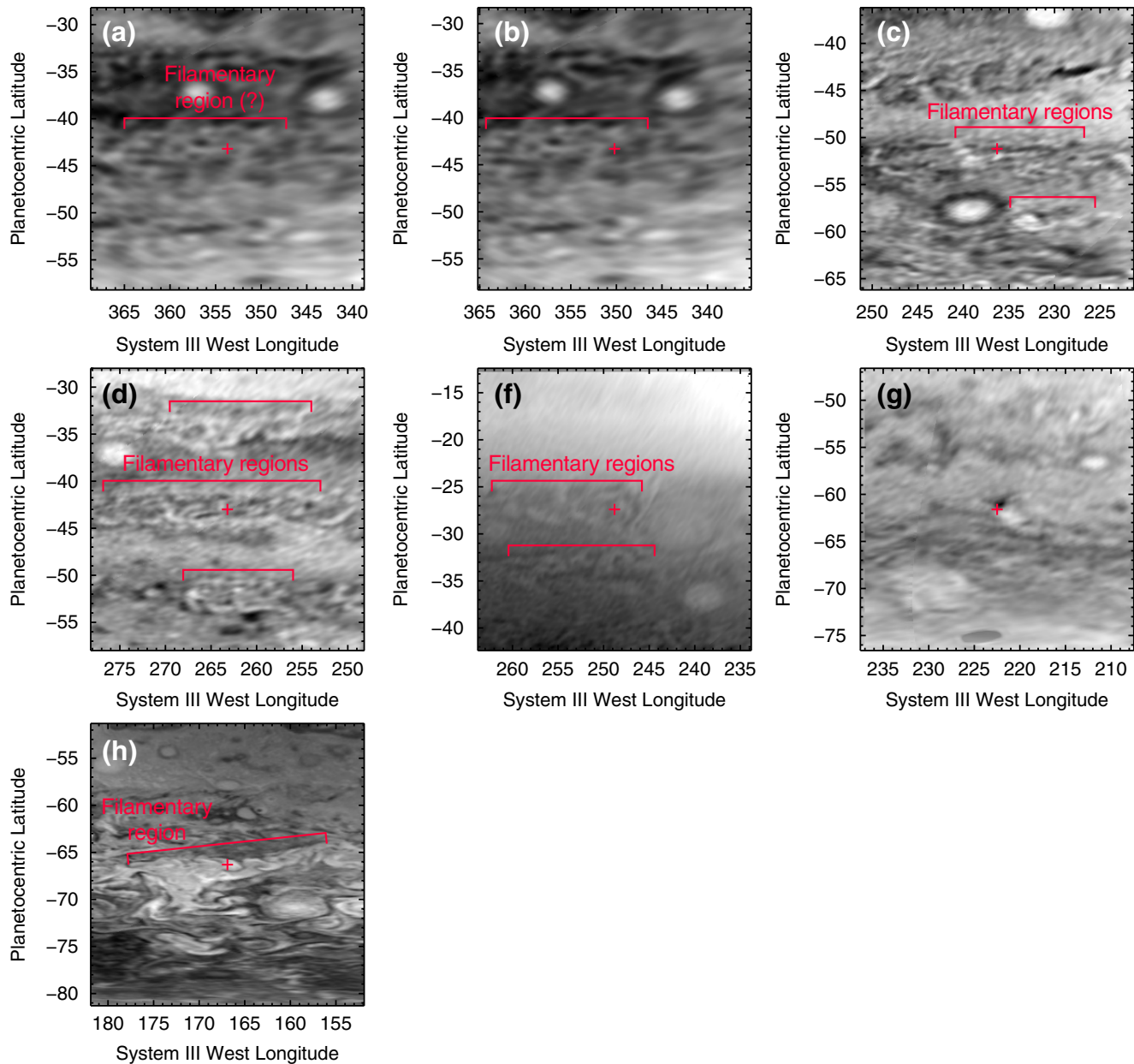


Figure 7. JunoCam images of Jupiter for the locations of seven of the bright flashes. The labels relate the JunoCam images to the bright flashes described in Table 1. In each case, the JunoCam data were obtained during the same perijove as the bright flash observation, and they were mostly obtained during the departure sequence as the spacecraft was moving away from the planet. The images shown here were made by combining data from the red and green JunoCam filters, obtained from the Planetary Data System (see the [Data Availability Statement](#)). The locations of the bright flashes are shown by the red crosses and the folded filamentary regions are marked by the lines. The geometry of the orbit means that there is no daylight JunoCam image for the location of flash (e). Processed JunoCam images for (i), (j) and (k) are not yet available. A higher resolution image of the region around flash (f) is shown in Figure 8.

122-ms observations once per second (Kolmasová et al., 2018). The chance of this timing and “field-of-view” coinciding with the timing, latitude and longitude of the UVS measurements is low. The MWR instrument has detected many lightning sferics in its 600 MHz channel (Brown et al., 2018), but the difference in the fields of views of MWR and UVS mean that they cannot observe the same point on the planet at the same time. The field of view of the 600 MHz MWR antenna is 120° from the UVS field of view, so as the spacecraft rotates it observes a given point ~20 s before and then ~10 s after UVS. This time gap is much larger than the expected time gap between lightning flashes and the associated elves or sprites, which is on the order of microseconds and milliseconds respectively (Rodger, 1999). The same issue affects comparisons between

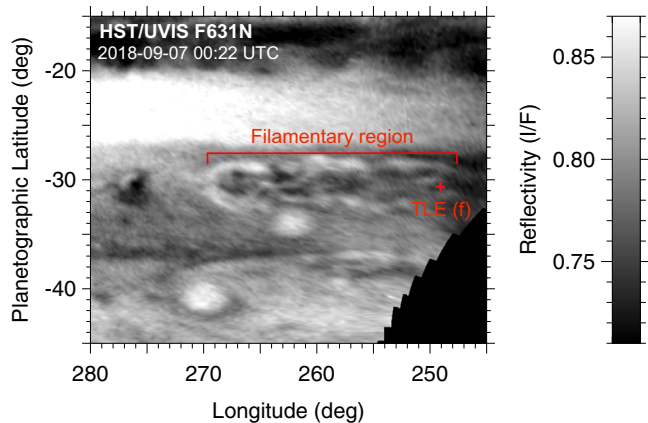


Figure 8. HST WFC3 image of Jupiter, obtained 5 h before bright flash (f) was observed. The scale gives the equivalent disk-center reflectivity after correction for limb darkening. The latitude and longitude of bright flash (f) is marked by the red cross. HST WFC3, Hubble Space Telescope Wide Field Camera 3.

UVS and the SRU visible light camera, which has a similar field of view to the 600 MHz MWR antenna.

While there are no direct observations to link the bright flashes with tropospheric lightning, we do note that they occur in regions of the planet where we would expect lightning to be present. Table 1 lists whether the wind shear at the latitude of each observation is cyclonic or anticyclonic; vorticities were obtained from Hubble Space Telescope observations (Tollefson et al., 2017; Wong et al., 2020). Out of the 10 observations for which wind shear could be measured, nine occurred at latitudes with cyclonic zonal wind shear. This is consistent with the bright flashes being caused by lightning, because lightning on Jupiter is more frequently observed in the cyclonic belts than in the anticyclonic zones (Brown et al., 2018; Little et al., 1999).

Further evidence comes from Figures 7 and 8, which show images of Jupiter obtained using JunoCam and the Hubble Space Telescope respectively. JunoCam is the outreach camera on the Juno mission and it visible-light wide-angle imaging during each PJ (Hansen et al., 2017). Figure 7 shows JunoCam images for 7 out of the 11 bright flashes; because of the geometry of the orbit, no dayside images of region near flash (e) were obtained, and processed JunoCam data for flashes (i), (j),

and (k) are not yet available from NASA's Planetary Data System (PDS). Figure 8 shows an image obtained using the Hubble Space Telescope Wide Field Camera 3 (HST WFC3) within 5 h of flash (f) and covering the longitude and latitude of the flash (Wong et al., 2020). Figures 7 and 8 show that several of the bright flashes occurred within folded filamentary regions, oblong cyclonic regions containing fine-scale filamentary structure (Morales-Juberías et al., 2002). Many previous lightning detections have been traced to cyclonic regions (Vasavada & Showman, 2005; Wong et al., 2020), or to regions that share the three cloud structure elements of active moist convection: high/thick convective towers, deep water clouds, and cloud-free clearings (Gierasch et al., 2000; Imai et al., 2020).

As the Juno mission continues, the UVS instrument will continue to be used to search for TLEs in Jupiter's atmosphere. More observations will increase the probability that there is an overlap with the Waves instrument observations, and will also allow us to conduct a statistical analysis of the occurrence rate and spatial distribution of our observations. Any observations made closer in to the planet will also help us to constrain the width of the bright flashes, which in turn will help to discriminate between sprites, sprite halos, and elves.

Data Availability Statement

The Juno UVS and JunoCam data used in this paper are archived in NASA's Planetary Data System (PDS). The Juno UVS data are available at the PDS Atmospheres Node: https://pds-atmospheres.nmsu.edu/PDS/data/jnouvs_3001 (Trantham, 2014). The JunoCam data are available at the PDS Imaging Node: <https://pds-imaging.jpl.nasa.gov/data/juno> (Caplinger, 2014). The HST observations are archived at the Mikulski Archive for Space Telescopes: <https://archive.stsci.edu/hlsp/wfcj> (Wong et al., 2020). The data used to produce the figures in this paper are available in Giles (2020).

References

- Baines, K. H., Simon-Miller, A. A., Orton, G. S., Weaver, H. A., Lunsford, A., Momary, T. W., et al. (2007). Polar lightning and decadal-scale cloud variability on Jupiter. *Science*, 318(5848), 226–229.
- Becker, H. N., Alexander, J. W., Atreya, S. K., Bolton, S. J., Brennan, M. J., Brown, S. T., et al. (2020). Small lightning flashes from shallow electrical storms on Jupiter. *Nature*, 584, 55.
- Benilan, Y., Smith, N., Jolly, A., & Raulin, F. (2000). The long wavelength range temperature variations of the mid-UV acetylene absorption coefficient. *Planetary and Space Science*, 48(5), 463–471.
- Bolton, S. J., Lunine, J., Stevenson, D., Connerney, J. E. P., Levin, S., Owen, T. C., et al. (2017). The Juno Mission. *Space Science Reviews*, 213, (1–4), 5–37.

Acknowledgments

We are grateful to NASA and contributing institutions, which have made the Juno mission possible. We thank Thomas Momary for advice on processing the JunoCam images. This work was funded by NASA's New Frontiers Program for Juno via contract with the Southwest Research Institute.

- Bonfond, B., Gladstone, G., Grodent, D., Gerard, J.-C., Greathouse, T., Hue, V., et al. (2018). Bar code events in the Juno-UVS data: Signature 10 MeV electron microbursts at Jupiter. *Geophysical Research Letters*, *45*(22), 12–108.
- Bonfond, B., Gladstone, G. R., Grodent, D., Greathouse, T. K., Versteeg, M. H., Hue, V., et al. (2017). Morphology of the UV aurorae Jupiter during Juno's first perijove observations. *Geophysical Research Letters*, *44*(10), 4463–4471.
- Borucki, W. J., & Magalhaes, J. A. (1992). Analysis of Voyager 2 images of jovian lightning. *Icarus*, *96*(1), 1–14.
- Borucki, W. J., & Williams, M. A. (1986). Lightning in the jovian water cloud. *Journal of Geophysical Research*, *91*(D9), 9893–9903.
- Brown, S., Janssen, M., Adumitroaie, V., Atreya, S., Bolton, S., Gulkis, S., et al. (2018). Prevalent lightning sferics at 600 megahertz near Jupiter's poles. *Nature*, *558*(7708), 87–90.
- Caplinger, M. (2014). *JUNO-J-JUNOCAM-2-EDR-L0-V1.0*. NASA Planetary Data System.
- Chen, F., & Wu, C. R. (2004). Temperature-dependent photoabsorption cross sections in the VUV-UV region. I. methane and ethane. *Journal of Quantitative Spectroscopy and Radiative Transfer*, *85*(2), 195–209.
- Chern, J. L., Hsu, R.-R., Su, H.-T., Mende, S. B., Fukunishi, H., Takahashi, Y., & Lee, L.-C. (2003). Global survey of upper atmospheric transient luminous events on the ROCSAT-2 satellite. *Journal of Atmospheric and Solar-Terrestrial Physics*, *65*(5), 647–659.
- Cook, A. F., Duxbury, T. C., & Hunt, G. E. (1979). First results on jovian lightning. *Nature*, *280*(5725), 794.
- Dubrovina, D., Luque, A., Gordillo-Vazquez, F. J., Yair, Y., Parra-Rojas, F. C., Ebert, U., & Price, C. (2014). Impact of lightning on the lower ionosphere of Saturn and possible generation of halos and sprites. *Icarus*, *24*-1, 313–328.
- Dubrovina, D., Nijdam, S., van Veldhuizen, E. M., Ebert, U., Yair, Y., & Price, C. (2010). Sprite discharges on Venus and Jupiter-like planets: A laboratory investigation. *Journal of Geophysical Research: Space Physics*, *115*(A6).
- Dyudina, U. A., Del Genio, A. D., Ingersoll, A. P., Porco, C. C., West, R. A., Vasavada, A. R., & Barbara, J. M. (2004). Lightning on Jupiter observed in the Ha line by the Cassini imaging science subsystem. *Icarus*, *172*(1), 24–36.
- Dyudina, U. A., Ingersoll, A. P., Ewald, S. P., Porco, C. C., Fischer, G., Kurth, W. S., & West, R. A. (2010). Detection of visible lightning on Saturn. *Geophysical Research Letters*, *37*(9).
- Franz, R. C., Nemzek, R. J., & Winckler, J. R. (1990). Television image of a large upward electrical discharge above a thunderstorm system. *Science*, *249*(4964), 48–51.
- Gerard, J.-C., Bonfond, B., Mauk, B. H., Gladstone, G. R., Yao, Z. H., Greathouse, T. K., et al. (2019). Contemporaneous observations of Jovian energetic auroral electrons and ultraviolet emissions by the Juno spacecraft. *Journal of Geophysical Research: Space Physics*, *124*(11), 8298–8317.
- Gierasch, P. J., Ingersoll, A. P., Banfield, D., Ewald, S. P., Helfenstein, P., SimonMiller, A., et al. (2000). Observation of moist convection in Jupiter's atmosphere. *Nature*, *403*(6770), 628–630.
- Giles, R. (2020). Possible transient luminous events observed in Jupiter's upper atmosphere. Mendeley Data, V2. <https://doi.org/10.17632/7bnpfb623x.2>
- Gladstone, G. R., Greathouse, T. K., Versteeg, M. H., Hue, V., Kammer, J. A., Davis, M. W., et al. (2019). Recent Juno-UVS observations of Jupiter's auroras. In *EPSC/DPS Joint Meeting Abstracts* (Vol. 13). Retrieved from <https://meetingorganizer.copernicus.org/EPSC-DPS2019/EPSC-DPS2019-794-1.pdf>
- Gladstone, G. R., Persyn, S. C., Eterno, J. S., Walther, B. C., Slater, D. C., Davis, M. W., et al. (2017). The ultraviolet spectrograph on NASA's Juno mission. *Space Science Reviews*, *213*(1–4), 447–473.
- Gladstone, G. R., Versteeg, M. H., Greathouse, T. K., Hue, V., Davis, M. W., Gerard, J.-C., et al. (2017). Juno-UVS approach observations of Jupiter's auroras. *Geophysical Research Letters*, *44*(15), 7668–7675.
- Gordillo-Vazquez, F. J., Luque, A., & Simek, M. (2011). Spectrum of sprite halos. *Journal of Geophysical Research*, *116*(A9).
- Gordillo-Vazquez, F. J., Passas, M., Luque, A., Sánchez, J., Van der Velde, O. A., & Montanyá, J. (2018). High spectral resolution spectroscopy of sprites: A natural probe of the mesosphere. *Journal of Geophysical Research: Atmospheres*, *123*(4), 2336–2346.
- Greathouse, T. K., Gladstone, G. R., Davis, M. W., Slater, D. C., Versteeg, M. H., Persson, K. B., et al. (2013). Performance results from in-flight commissioning of the Juno Ultraviolet Spectrograph (Juno-UVS). In *Uv, x-ray, and gamma-ray space instrumentation for astronomy xviii* (Vol. 8859, p. 88590T). <https://doi.org/10.1117/12.2024537>
- Gurnett, D. A., Shaw, R. R., Anderson, R. R., Kurth, W. S., & Scarf, F. L. (1979). Whistlers observed by Voyager 1: Detection of lightning on Jupiter. *Geophysical Research Letters*, *6*(6), 511–514.
- Gustin, J., Feldman, P. D., Gerard, J.-C., Grodent, D., Vidal-Madjar, A., Jaffel, L. B., et al. (2004). Jovian auroral spectroscopy with FUSE: Analysis of self-absorption and implications for electron precipitation. *Icarus*, *171*(2), 336–355.
- Hansen, C. J., Caplinger, M. A., Ingersoll, A., Ravine, M. A., Jensen, E., Bolton, S., & Orton, G. (2017). Junocam: Juno's outreach camera. *Space Science Reviews*, *213*(1–4), 475–506.
- Hue, V., Gladstone, G. R., Greathouse, T. K., Kammer, J. A., Davis, M. W., Bonfond, B., et al. (2019). In-flight characterization and calibration of the Juno-ultraviolet spectrograph (Juno-UVS). *The Astronomical Journal*, *157*(2), 90.
- Hue, V., Greathouse, T., Bonfond, B., Saur, J., Gladstone, G., Roth, L., et al. (2019). Juno-UVS observation of the Io footprint during solar eclipse. *Journal of Geophysical Research: Space Physics*, *124*(7), 5184–5199.
- Imai, M., Santolik, O., Brown, S. T., Kolmasova, I., Kurth, W. S., Janssen, M. A., et al. (2018). Jupiter lightning-induced whistler and sferic events with Waves and MWR during Juno perijoves. *Geophysical Research Letters*, *45*(15), 7268–7276.
- Imai, M., Wong, M. H., Kolmasova, I., Brown, S. T., Santolik, O., Kurth, W. S., et al. (2020). High-spatiotemporal resolution observations of Jupiter lightning-induced radio pulses associated with sferics and thunderstorms. *Geophysical Research Letters*, *47*(15), e2020GL088397.
- Kammer, J. A., Hue, V., Greathouse, T. K., Gladstone, G. R., Davis, M. W., & Versteeg, M. H. (2018). Planning operations in Jupiter's high-radiation environment: Optimization strategies from Juno-UVS. In *Space telescopes and instrumentation 2018: Ultraviolet to gamma ray* (Vol. 10699, p. 106993A). <https://doi.org/10.1117/12.2312261>
- Kanmae, T., Stenbaek-Nielsen, H. C., & McHarg, M. G. (2007). Altitude resolved sprite spectra with 3 ms temporal resolution. *Geophysical Research Letters*, *34*(7).
- Kolmasova, I., Imai, M., Santolik, O., Kurth, W. S., Hospodarsky, G. B., Gurnett, D. A., et al. (2018). Discovery of rapid whistlers close to Jupiter implying lightning rates similar to those on earth. *Nature Astronomy*, *2*(7), 544–548.
- Lee, A. Y., Yung, Y. L., Cheng, B.-M., Bahou, M., Chung, C.-Y., & Lee, Y.-P. (2001). Enhancement of deuterated ethane on Jupiter. *The Astrophysical Journal Letters*, *551*(1), L93.
- Levin, Z., Borucki, W. J., & Toon, O. B. (1983). Lightning generation in planetary atmospheres. *Icarus*, *56*(1), 80–115.
- Little, B., Anger, C. D., Ingersoll, A. P., Vasavada, A. R., Senske, D. A., Breneman, H. H., et al. (1999). Galileo images of lightning on Jupiter. *Icarus*, *142*(2), 306–323.
- Luque, A., Dubrovina, D., Gordillo-Vazquez, F. J., Ebert, U., Parra-Rojas, F. C., Yair, Y., & Price, C. (2014). Coupling between atmospheric layers in gaseous giant planets due to lightning-generated electromagnetic pulses. *Journal of Geophysical Research: Space Physics*, *119*(10), 8705–8720.

- Markwardt, C. B. (2009). Non-linear least-squares fitting in IDL with MPFIT. In *Astronomical data analysis software and systems XVIII* (Vol. 411, p. 251). Retrieved from <http://adsabs.harvard.edu/full/2009ASPC..411..251M>
- Morales-Juberias, R., Sanchez-Lavega, A., Lecacheux, J., & Colas, F. (2002). A comparative study of jovian cyclonic features from a six-year (1994-2000) survey. *Icarus*, *160*(2), 325–335.
- Moses, J. I., Fouchet, T., Bezdard, B., Gladstone, G. R., Lellouch, E., & Feuchtgruber, H. (2005). Photochemistry and diffusion in Jupiter's stratosphere: Constraints from ISO observations and comparisons with other giant planets. *Journal of Geophysical Research*, *110*(E8).
- Pasko, V. P. (2010). Recent advances in theory of transient luminous events. *Journal of Geophysical Research*, *115*(A6).
- Perez-Invernon, F. J., Luque, A., & Gordillo-Vazquez, F. J. (2017). Three-dimensional modeling of lightning-induced electromagnetic pulses on Venus, Jupiter, and Saturn. *Journal of Geophysical Research: Space Physics*, *122*(7), 7636–7653.
- Pryor, W. R., Ajello, J. M., Tobiska, W. K., Shemansky, D. E., James, G. K., Hord, C. W., et al. (1998). Galileo ultraviolet spectrometer observations. *Journal of Geophysical Research*, *103*(E9), 20–149.
- Rinnert, K., Lanzerotti, L. J., Uman, M. A., Dehmel, G., Gliem, F. O., Krider, E. P., & Bach, J. (1998). Measurements of radio frequency signals from lightning in Jupiter's atmosphere. *Journal of Geophysical Research: Planets*, *103*(E10), 22979–22992.
- Rodger, C. J. (1999). Red sprites, upward lightning, and VLF perturbations. *Reviews of Geophysics*, *37*(3), 317–336.
- Sato, M., Ushio, T., Morimoto, T., Kikuchi, M., Kikuchi, H., Adachi, T., et al. (2015). Overview and early results of the global lightning and sprite measurements mission. *Journal of Geophysical Research: Atmospheres*, *120*(9), 3822–3851.
- Smith, B. A., Soderblom, L. A., Johnson, T. V., Ingersoll, A. P., Collins, S. A., Shoemaker, E. M., et al. (1979). The jupiter system through the eyes of Voyager 1. *Science*, *204*(4396), 951–972.
- Smith, P. L., Yoshino, K., Parkinson, W., Ito, K., & Stark, G. (1991). High-resolution, VUV (147–201 nm) photoabsorption cross sections for C₂H₂ at 195 and 295 K. *Journal of Geophysical Research: Planets*, *96*(E2), 17529–17533.
- Trantham, B. (2014). *JNO-J-UVS-3-RDR-V1.0*. NASA Planetary Data System.
- Tollefson, J., Wong, M. H., de Pater, I., Simon, A. A., Orton, G. S., Rogers, J. H., et al. (2017). Changes in Jupiter's zonal wind profile preceding and during the Juno mission. *Icarus*, *296*, 163–178.
- Vasavada, A. R., & Showman, A. P. (2005). Jovian atmospheric dynamics: An update after Galileo and Cassini. *Reports on Progress in Physics*, *68*(8), 1935.
- Vincent, M. B., Clarke, J. T., Ballester, G. E., Harris, W. M., West, R. A., Trauger, J. T., et al. (2000). Jupiter's polar regions in the ultraviolet as imaged by HST/WFPC2: Auroral-aligned features and zonal motions. *Icarus*, *143*(2), 205–222.
- Wong, M. H., Simon, A. A., Tollefson, J. W., de Pater, I., Barnett, M. N., Hsu, A. I., et al. (2020). High-resolution UV/optical/IR imaging of Jupiter in 2016-2019. *The Astrophysical Journal Supplement Series*, *247*(2), 58.
- Yair, Y., Takahashi, Y., Yaniv, R., Ebert, U., & Goto, Y. (2009). A study of the possibility of sprites in the atmospheres of other planets. *Journal of Geophysical Research*, *114*(E9).
- Zarka, P., & Pedersen, B. M. (1986). Radio detection of Uranian lightning by Voyager 2. *Nature*, *323*(6089), 605–608.